Published OnlineFirst October 15, 2015; DOI: 10.1158/0008-5472.CAN-14-3373

Microenvironment and Immunology

Cancer Research

Macrophage Blockade Using CSF1R Inhibitors Reverses the Vascular Leakage Underlying Malignant Ascites in Late-Stage Epithelial Ovarian Cancer

Diana L. Moughon[1], Huanhuan He[2], Shiruyeh Schokrpur[1], Ziyue Karen Jiang[1,3], Madeeha Yaqoob[4], John David[5], Crystal Lin[1], M. Luisa Iruela-Arispe[6,7,8], Oliver Dorigo[2], and Lily Wu[1,3,8]

Abstract

Malignant ascites is a common complication in the late stages of epithelial ovarian cancer (EOC) that greatly diminishes the quality of life of patients. Malignant ascites is a known consequence of vascular dysfunction, but current approved treatments are not effective in preventing fluid accumulation. In this study, we investigated an alternative strategy of targeting macrophage functions to reverse the vascular pathology of malignant ascites using fluid from human patients and an immunocompetent murine model (ID8) of EOC that mirrors human disease by developing progressive vascular disorganization and leakiness culminating in massive ascites. We demonstrate that the macrophage content in ascites fluid from human patients and the ID8 model directly correlates with vascular permeability. To further substantiate macrophages' role in the pathogenesis of malignant ascites, we blocked macrophage function in ID8 mice using a colony-stimulating factor 1 receptor kinase inhibitor (GW2580). Administration of GW2580 in the late stages of disease resulted in reduced infiltration of protumorigenic (M2) macrophages and dramatically decreased ascites volume. Moreover, the disorganized peritoneal vasculature became normalized and sera from GW2580-treated ascites protected against endothelial permeability. Therefore, our findings suggest that macrophage-targeted treatment may be a promising strategy toward a safe and effective means to control malignant ascites of EOC. *Cancer Res; 75(22); 4742–52. ©2015 AACR.*

Introduction

Malignant ascites is a common side effect of epithelial ovarian cancer (EOC), characterized by the accumulation of fluid in the abdomen (1). It has been estimated that approximately 70% of patients with EOC will develop ascites, particularly in the disseminated or recurrence stage of the disease. Although it is debated whether malignant ascites contributes to a poor prognosis or is merely indicative of the advanced stage of progression for patients with EOC, this complication clearly compromises their quality of life (2). Current treatment methods, such as paracentesis and peritovenous shunts, physically drain the accumulated ascites fluid but do not address the root cause of this complication. Hence, the ascites fluid reaccumulates after the procedure. Furthermore, a significant risk of side effects due to infection or fluid and electrolyte imbalance are associated with physical drainage of malignant ascites (1, 2).

In the pursuit of new, effective pharmaceutical remedies to manage ascites of EOC, vascular endothelial growth factor (VEGF) emerged as an excellent target for several reasons (3, 4). VEGF, also known as vascular permeability factor, was originally isolated from ascites fluid (5). VEGF is markedly elevated in the ascites fluid of ovarian cancer patients and increased VEGF expression is a poor prognostic marker for EOC (6–10). In xenograft mouse EOC models, anti-VEGF treatments effectively suppressed tumor growth and reduce ascites formation (11, 12). Corroborating these preclinical findings are two recent phase II clinical trials showing that treatment with VEGF trap Aflibercept significantly reduces ascites buildup in patients with advanced ovarian cancer (13, 14). However, the enthusiasm for this VEGF blockade treatment is dampened by significant treatment-related adverse vascular events, such as hypertension, venous thrombosis, and congestive heart failure. The most concerning of the adverse events is fatal intestinal perforation, which affected 10% of Aflibercept-treated patients in the randomized, controlled study (14). Therapies with anti-VEGF

[1]Department of Molecular and Medical Pharmacology, University of California Los Angeles, Los Angeles, California. [2]Department of Obstetrics and Gynecology, Division of Gynecologic Oncology, Stanford University School of Medicine, Stanford, California. [3]Department of Urology, David Geffen School of Medicine, University of California Los Angeles, Los Angeles, California. [4]Department of Surgery and Cancer, Hammersmith hospital, Imperial College London, London, United Kingdom. [5]Department of Molecular and Medical Pharmacology, California Nanosystems Institute, Los Angeles, California. [6]Department of Molecular, Cell and Developmental Biology, Los Angeles, California. [7]Molecular Biology Institute, University of California Los Angeles, Los Angeles, California. [8]Jonsson Comprehensive Cancer Center, University of California Los Angeles, Los Angeles, California.

Note: Supplementary data for this article are available at Cancer Research Online (http://cancerres.aacrjournals.org/).

Corresponding Author: Lily Wu, University of California, Los Angeles, CHS 33-118 Box 951735, 650 Charles Young Dr. South, Los Angeles, CA 90095. Phone: 310-794-4390; Fax: 310-825-6267; E-mail: lwu@mednet.ucla.edu

doi: 10.1158/0008-5472.CAN-14-3373

Published OnlineFirst October 15, 2015; DOI: 10.1158/0008-5472.CAN-14-3373

antibody, bevacizumab, also have similar severe side effects (15). These life-threatening side effects of VEGF-targeted therapies raise significant concerns of their use without clear long-term survival benefits. The search for safe and effective treatments to manage malignant ascites of EOC continues.

Another tumor microenvironment component that has received great attention in recent years is the infiltrating myeloid cells, such as macrophages (16). A large volume of evidence supports that once recruited to and "educated" by the tumor, these macrophages promote cancer progression (17) by various mechanisms such as heightening the immunosuppressive conditions, angiogenesis, and tissue remodeling, which in turn leads to enhanced tumor growth and metastasis (16, 17). The tumor-promoting tumor-associated macrophages (TAM) are commonly designated as "M2" in contrast to the classical-activated inflammatory "M1" macrophages (16, 17). In EOC, a large infiltrating population of macrophages has been observed within tumor nodules and in the ascites fluid (18, 19). However, their phenotypes and functions have not been well studied. A distinctive feature of many human EOC tumors is that they secrete copious amounts of colony-stimulating factor 1 (CSF-1). CSF-1, also known as M-CSF, is a critical cytokine that regulates the differentiation, growth, and function of macrophages by binding to and activating its cognate receptor CSF1R (*c-fms*) present on monocytes and macrophages (20). CSF-1 is also known to play a role in educating macrophages into M2 macrophages (21, 22). Not only is CSF-1 known to be elevated in patient ascites, but an elevated level of this cytokine is associated with poor prognosis (23, 24). These findings suggest that the CSF-1/CSF1R axis might promote oncogenic effects on tumor cells directly or modulate tumorigenesis through the recruitment and function of TAMs found in EOC tumors, or both.

In this study, we characterized the progression of the murine ID8 EOC model with special attention paid to the evolution of TAMs in this context. Mirroring the characteristics of human EOC, the ID8 tumor-bearing mice developed massive malignant ascites in the late stages. We observed a great expansion in macrophages within the ascites that correlated with vascular dysregulation. To demonstrate a causative role of TAMs in the vascular pathology of malignant ascites, we used a selective CSF1R kinase inhibitor, GW2580, to block macrophage function. GW2580 lowered "M2" TAMs and also dramatically reduced ascites fluid accumulation. Findings from this study support the notion that TAMs are key players in causing or perpetuating the vascular leakiness of EOC ascites.

Materials and Methods

Cell culture, lentiviral cell marking, and RT-PCR

All cell lines were cultured at 37°C with 5% CO_2 in DMEM with 100 U/mL penicillin and specific media components for each cell line as follows. Murine ID8 EOC cells (kind gift from Dr. Oliver Dorigo, Stanford University, Stanford, CA) require 4% FBS and 1% insulin–transferrin–selenium (ITS, Gibco 100× solution). Immortomice-derived endothelial cells (IMEC) from liver sinusoidal endothelial cells (EC) required 10% FBS and 20 U/mL interferon-gamma (IFNγ), whereas OVCAR3 cells required 20% FBS and SVEC4-10 cells required 10% FBS. Human umbilical vein endothelial cells (HUVEC) required MCDB-131 medium (VEC Technologies) with 10% FBS. Cell lines were PCR tested for the absence of mycoplasma contamination.

Renilla luciferase lentiviral vector was propagated as previously described (25). ID8 cells were transduced at multiplicity of infection 2, which resulted in 97% GFP^+ transduction.

In vivo tumor models and bioluminescent imaging

All animal experiments were approved by the UCLA Institutional Animal Care and Use Committee and conformed to national animal care guidelines, ethics, and regulations. For the intraperitoneal model: *Renilla* luciferase-marked ID8 cells (10×10^6) in 500 μL PBS were injected intraperitoneally into C57BL/6 female mice (Jackson Laboratory, Bar Harbor, ME). GW2580 (LC Labs) treatment (160 mg/kg) or control diluent (0.1% hydroxypropyl methylcellulose; Sigma-Aldrich; 0.1% Tween20 in distilled H_2O) was given daily starting 10 to 12 weeks after tumor injection.

For the OVCAR3 model, cells were initially grown subcutaneously in female nude mice (Jackson Laboratories) to obtain enough tumor cells. Tumors were harvested and cells disassociated, and 2.5×10^6 cells were injected intraperitoneally into female nude mice. Animals develop signs of late-stage EOC after 3 months, and GW2580 treatment or diluent was given as described above.

Renilla-marked ID8 tumor-bearing mice were imaged using the IVIS Lumina II as previously described (25), and bioluminescent signals were analyzed using Living Image 4.0 software.

Perfusion assay and whole mount immunohistochemistry

Mice were injected intravenous with 60 μg biotinylated lectin (Vector) and 60 μg streptavidin Cy3 (Invitrogen). After 5 minutes, mice were anesthetized and perfused with 20 mL of PBS and 20 mL of 3% paraformaldehyde injected into the left ventricle.

Tissues were fixed with 2% PFA for 5 to 6 hours, then washed with PBS overnight at 4°C. Mesentery was fragmented into 0.2 to 0.5 cm and blocked in PBST (0.05% Tween20 in PBS) with 3% donkey serum for 30 minutes. Samples were then incubated with primary antibodies for 1 hour and washed with PBST, followed by secondary antibodies (1:200) for 1 hour. Antibodies used are antimouse CD31 (1:50; BD Biosciences), antimouse isolectin (1:75; Invitrogen), antimouse CD11b (1:50; BD Biosciences), and antimouse CD206 (1:50; BD Biosciences).

Miles assay

One microgram of Evans Blue in 100 μL sterile PBS was intravenously injected into mice. After 30 minutes, mice were sacrificed and mesentery tissue was removed. Tissue was weighed and placed in 500 μL formamide for 48 hours at 55°C. The optical density of the extracted Evans Blue was read at 620 nm (BioTek Synergy H1 plate reader) and converted to ng/mg tissue.

Flow cytometry

Harvested tumors were minced into fragments and digested with 80 U/mL collagenase (Invitrogen) in PBS containing 2% FBS for 1 hour at 37°C, and passed through a 70 μm cell strainer (BD). Spleens and lymph nodes were gently dissociated between the rough surfaces of two glass slides. Peripheral blood was obtained by retro orbital bleed. Ascites was completely drained from the peritoneum with a syringe. After red blood cell lysis (Sigma-Aldrich), single-cell suspensions were filtered and incubated for 30 minutes on ice with the following: APC-CD45, e450-CD11b, PerCP-Cy5.5-Gr-1, PE-Cy7-F4/80, a700-MHCII, PE-CD4, e450-CD8, and FITC-CCR2 (eBioscience, 1:500). Intracellular staining was performed for PE-Cy7-IFNγ and PE-IL12. Samples were run on

Published OnlineFirst October 15, 2015; DOI: 10.1158/0008-5472.CAN-14-3373

the BD LSR-II flow cytometer (BD). Data were analyzed with FlowJo software (TreeStar).

Processing of patient samples

Patient materials were collected under a UCLA Gyn-Onc Tissue Bank protocol approved by the Institutional Review Board. All patients' identification was blinded in this study. Fifty milliliters of freshly harvested ascites fluid were spun down at 1500 rpm and sera were frozen immediately at −80°C. Ascites cells were subjected to red blood cell lysis, filtered, and incubated for 30 minutes in ice with the following flow cytometry antibodies: PE-Cy7-CD33, PE-CD68, APC-HLA-DR, FITC-CD4, APC-e780-CD8a (eBioscience, 1:500), PerCP e710-CD206, Alexa Fluor 488-Muc-1 (eBioscience, 1:200). Cells were fixed for 15 minutes in 3% PFA at RT and run on the BD LSR-II flow cytometer (BD). Data were analyzed with FlowJo software (TreeStar).

In vitro permeability assays

Liver sinusoidal ECs from IMEC and HUVECs were plated on stabilized 8W10E+ PET Electric Cell-substrate Impedance Sensing (ECIS) Cultureware Disposable Electrode Arrays (Applied Biophysics). Three hundred microliters of murine serum was added to each well-containing confluent IMEC and 300 μL patient serum was added to each well-containing confluent HUVECs. Arrays were connected to and read by an ECIS 1600R instrument (Applied Biophysics) for four hours. Values recorded are in terms of resistance to permeability. Data were analyzed using ECIS software (Applied Biophysics) and GraphPad Prism (GraphPad Software).

SVEC4-10 murine lymphatic ECs were incubated in normal media or media with 5% ascites sera for 24 hours. Cells were then collected, fixed in 3% PFA for 15 minutes, permeabilized with 90% methanol for 30 minutes, and stained according to our flow cytometry protocol with Alexa Fluor 488 anti-VE-Cadherin (1:100; eBioscience).

Statistical analysis

Data are presented as mean plus or minus SEM. Statistical comparisons between groups were performed using the Student *t* test.

Results

The ID8 murine EOC model mirrors late stages of human disease with malignant ascites

The ID8 is a well-studied murine serous EOC model (26–28). The full complement of immune system of this model is particularly favorable to investigate the innate immune response of the myeloid cells. The ID8 cells were marked with *Renilla* luciferase, enabling longitudinal monitoring of tumor growth and dissemination by noninvasive bioluminescent imaging. For the intraperitoneal model, bioluminescent signals from the tumor cells first became detectable at around week 9 postinjection, which also corresponded to the time that ascites began to accumulate (Fig. 1A), and the tumors grew rapidly from this point onward. By week 12, the tumors had grown throughout the peritoneal cavity (Fig. 1A) and ascites greatly distended the abdomen. The substantial ascites found in each mouse was hemorrhagic and tumor nodules had spread to the mesenteries, peritoneal wall, liver, and fat pads (Supplementary Fig. S1A). The same pattern of peritoneal dissemination and ascites formation were also observed in the orthotopic ID8 model, implanted into the ovarian bursa (Supplementary Fig. S1B). Taken together, both the intraperitoneal and intrabursal ID8 model recapitulate important characteristics of human EOC with slow initial growth that progressed to dispersed peritoneal metastasis, and massive ascites.

Immune and vascular dysregulation worsen as EOC progresses

Immune dysregulation in patients with cancer often results in the systemic expansion of myeloid cell populations that can be observed in the peripheral blood, lymphoid organs, and at the tumor (29). This expansion of circulating and infiltrating myeloid cells is also associated with worse prognosis (16). Consistent with this finding, we observed the progressive increase in the immature myeloid cells also known as myeloid-derived suppressor cells (MDSC) in the peripheral blood in the ID8 model from weeks 6 to 12 after tumor injection (Supplementary Fig. S1C). Increases of MDSCs and macrophages in the spleen and lymph nodes (data not shown) and splenomegaly (Supplementary Fig. S1D) were also observed consistently. The systemic expansion of the myeloid population was also manifested in the tumor, resulting in a significant increase in TAM content over time (Supplementary Fig. S1E).

Next we analyzed the immune cell content in the ascites fluid and found that macrophages and floating tumor cells were the majority of viable cells in the ascites fluid at both week 10 (the eventual start time of treatments) and week 12 (Fig. 1B). The immune cells in ID8 ascites consist of a high proportion of immunosuppressive and protumorigenic subtype, as the MHCII− M2 to MHCII+ M1 macrophage and CD4 to CD8 T-cell ratios were both around 3 to 1 at week 12, an increase from the ratios at week 10 (Fig. 1C). Large numbers of macrophages and a high ratio of CD4 to CD8 T cell infiltration have previously been associated with poor prognosis in breast cancer (30). We modified this immune cell signature by including the cell ratio of M2 to M1 macrophages in the ascites fluid.

The hemorrhagic nature of the ascites in the ID8 model indicates that vascular leakage and extravasation of red blood cells is occurring. Hence, the ID8 tumor-bearing mice developed severe anemia in the late stages of the disease (Fig. 1D). Close examination of mesentery blood vasculature revealed that by week 12 the vasculature was highly disorganized (Fig. 2A), with greatly increased vessel density (Fig. 2B), vessel width (Fig. 2C), and number of branch points (Fig. 2D). The *in vivo* vascular function in the animals was further examined with the Miles assay, which assess vascular leakage by the extravasation of Evans Blue dye from circulation into tissues, and a lectin perfusion assay. ID8 tumor-bearing mice displayed clear vascular leakage compared with naïve animals (Supplementary Fig. S1F). In contrast to the robust lectin perfusion observed in the mesentery capillaries of naïve animals, the vessel perfusion function in the mesentery capillaries of tumor-bearing mice was significantly decreased, to about 25% of normal (Fig. 2E). No notable difference in perfusion in the larger mesentery arterioles was observed between tumor-bearing and naïve animals (data not shown), indicating that the leakage of blood and ascites fluid is occurring at the capillary level. Parallel the dysregulated blood vasculature, tumor-bearing mice displayed increased lymphatic density in the mesentery (Supplementary Fig. S1G), and tortuous lymphatics with enlarged lumen (Supplementary Fig. S1H). Although these findings are consistent with known lymphatic vascular and lymph drainage dysfunction in EOC malignant ascites (31, 32), they require further functional

Published OnlineFirst October 15, 2015; DOI: 10.1158/0008-5472.CAN-14-3373

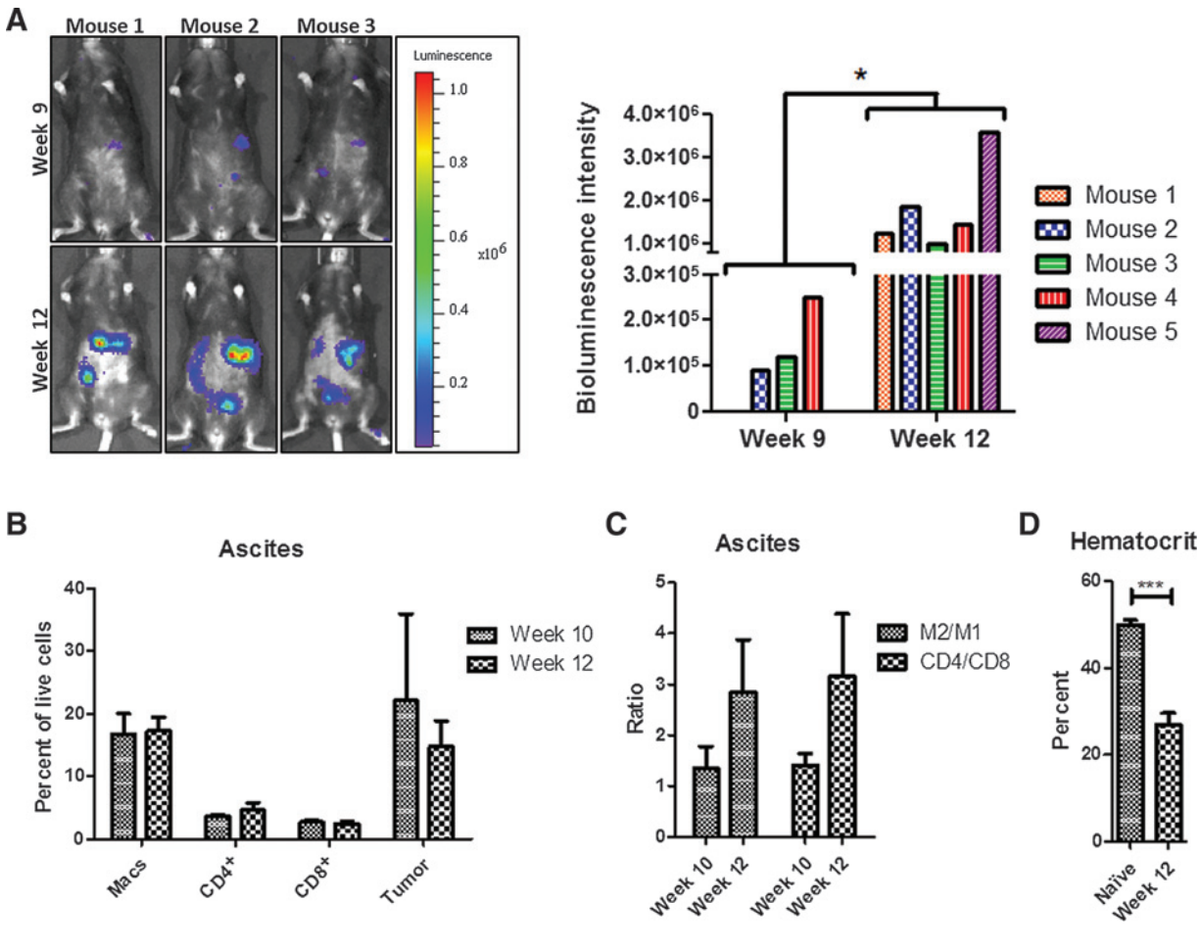

Figure 1.
Murine ID8 epithelial ovarian cancer model. A, bioluminescent imaging of three representative animals bearing intraperitoneal *Renilla* luciferase-marked ID8 tumor cells at 9 and 12 weeks posttumor implantation (left images). Right graph shows the maximum signal intensity (radiance = p/sec/cm^2/sr) in the peritoneal cavity ($n = 5$). B, proportion of specified cell types (CD45$^+$ F4/80$^+$ macrophages, CD4$^+$ and CD8$^+$ T cells, and GFP$^+$ tumor cells) found floating in the ascites as measured by flow cytometry at week 10 and week 12 posttumor cell implantation. C, ratios of M2 macrophages (CD45$^+$ F4/80$^+$ MHCII$^-$) to M1 macrophages (CD45$^+$ F4/80$^+$ MHCII$^+$) and CD4$^+$ T cells to CD8$^+$ T cells in the ascites at week 10 and week 12 posttumor cell implantation. D, severe anemia is seen in late stages of intraperitoneal ID8 model ($n = 3$–4). *, $P < 0.05$; ***, $P < 0.001$.

verification. Suffice to say, the preclinical data presented so far support that macrophages are playing a pivotal role in the pathogenesis of EOC malignant ascites. To further verify this assertion, we pursued a therapeutic approach to block macrophage function in the ID8 EOC model.

Suppressing macrophage function with CSF1R blockade ameliorated the vascular dysfunction of malignant ascites of EOC

Because the CSF-1/CSF1R axis is known to be a critical pathway in the development and function of myeloid cells and macrophages, we used a highly selective CSF1R inhibitor, GW2580 (33), to treat mice during the late stages of ID8 EOC. We and others have shown that GW2580 is able to selectively and effectively inhibit the protumorigenic functions of TAMs in several tumor models, including prostate, breast, and lung cancer (34–36). A confounding issue in EOC is that CSF-1 and CSF1R were found to be expressed in human ovarian cancer and this signaling pathway has been implicated to have a tumor-intrinsic role in promoting EOC oncogenesis (23). Although ID8 tumor cells express a moderate level of CSF-1 comparing to several other human EOC lines (Supplementary Fig. S2A), this model expresses negligible level of CSF1R that is more than 5 orders of magnitude below that expressed in a macrophage cell line and bone marrow derived macrophages (data not shown), and 5- to 10-fold lower than three other human ovarian cancer lines (Supplementary Fig. S2B). Furthermore, unlike macrophages, ID8 cells were not responsive to CSF1 induction or CSF1R blockade *in vitro* (34) (Supplementary Fig. S2C and S2D) and subcutaneous ID8 tumor growth was not affected by GW250 treatment (Supplementary Fig. S2E). There were also no off-target effects or organ toxicity with the treatment (Supplementary Fig. S2F; refs. 33, 34). Thus, we conclude that the therapeutic action of CSF1R inhibition is directed at macrophages and not at the ID8 tumor cells.

Female mice-bearing intraperitoneal implanted ID8 tumors were allowed to progress to late stage, when ascites developed, and then treated with diluent or GW2580 for 2 more weeks (Fig. 3A). Control diluent-treated mice continued to accumulate ascites

Published OnlineFirst October 15, 2015; DOI: 10.1158/0008-5472.CAN-14-3373

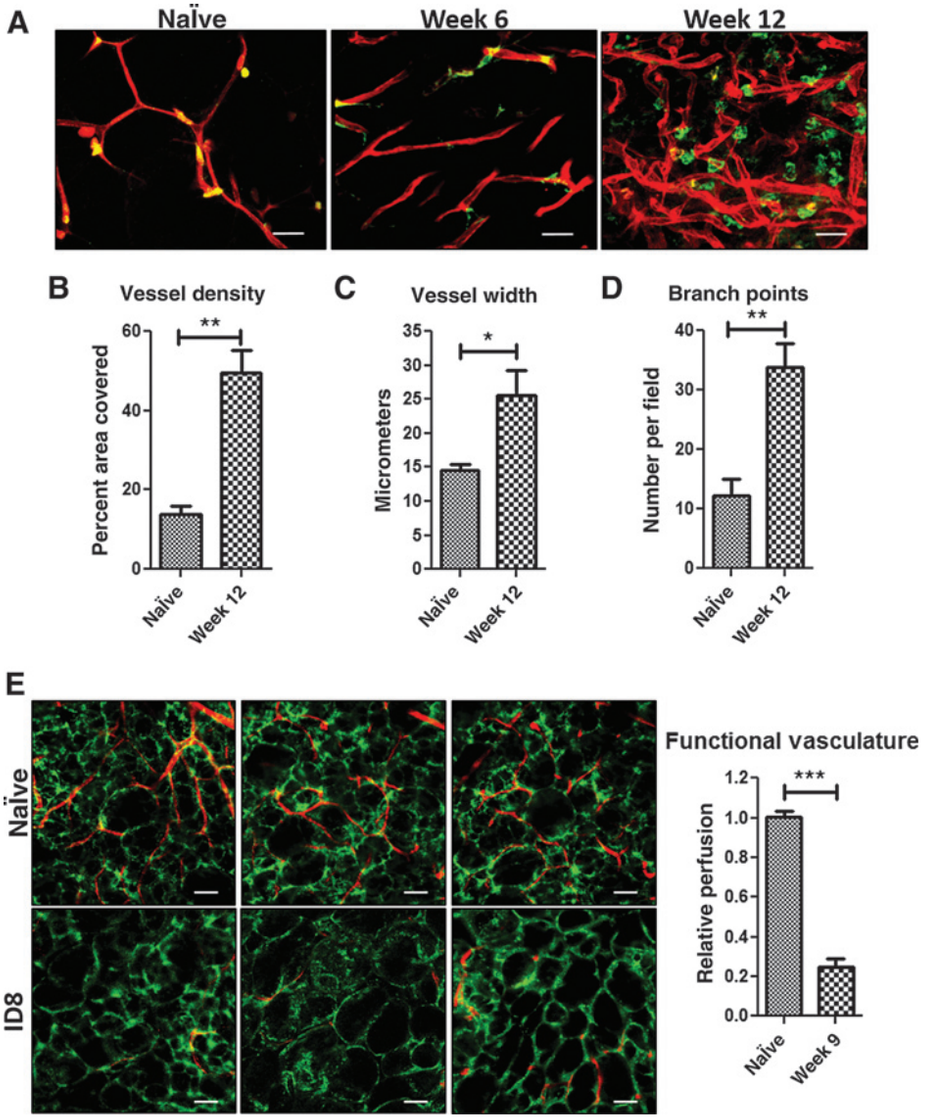

Figure 2.
Vascular deregulation in ID8 EOC. A, mesentery tissues isolated from the intestinal region were stained for vasculature (isolectin, red) and macrophages (CD11b in naïve or CD206 in tumor-bearing, green). B–D, vascular parameters such as vessel density, vessel width, and branch points, respectively, were scored in the mesentery tissues ($n = 4$). E, vasculature function assay with perfused lectin (red) and surface stained CD31 (green) assessed by whole mount. Quantification is the percentage of $CD31^+$ vessels that are also lectin+ and normalized to naïve mouse vasculature ($n = 2$–4). Scale bars, 50 μm. *, $P < 0.05$; **, $P < 0.01$; ***, $P < 0.001$.

whereas GW2580 treatment resulted in a significant reduction of ascites, down from an average volume of 6.2 mL/control animal to 1.9 mL/treated animal (Fig. 3B), and prevented the development of severe anemia (Fig. 3C). Notably, GW2580 treatment significantly altered the content of macrophages in the ascites. More than the 2 weeks of treatment course, the percentage of floating ascites macrophages in the control cohort increased significantly whereas those in the GW2580-treated ascites reduced significantly (Fig. 3D). For instance, in one experiment, the absolute number of M2 macrophages decreased from 41.9 ± 15.9 to 2.9 ± 1.7 million ($P < 0.05$), the absolute number of M1 macrophages was not significantly affected by the GW2580 treatment, and CD8 T cell increased from 0.68 ± 0.16 to 2.2 ± 1.4 million in ascites by GW2580 treatment (Fig. 3E, Supplementary Fig. S3A). Notably, the high 3:1 ratio of M2:M1 macrophage and CD4:CD8 T cell were reduced to approximately 1:1 by GW2580 treatment (Fig. 3F). Significantly more of the GW-treated ascites macrophages expressed CCR2 (Fig. 3G), and many more of those macrophages expressed IFNγ and IL12 compared with control ascites macrophages (Supplementary Fig. S3B and S3C). These results indicate that inhibiting macrophage function with CSF1R blockade was able to reverse the protumorigenic, immunosuppressive phenotypes of the ascites immune cells.

Given the significant reduction of ascites fluid volume, the critical issue to unveil is the impact of CSF1R blockade on the peritoneal vasculature. Upon staining of the mesentery blood vasculature, a clear normalization was seen in GW2580-treated mice (Fig. 4A). Along with the reduction in vessel density (Fig. 4B), there is a concomitant decrease in vessel width (Fig. 4C), tortuosity, and branch points (Fig. 4D). We further explored the blood vascular dysregulation in a second EOC model, namely the human OVCAR3 xenograft model. As seen in Fig. 4E, GW2580 treatment again normalized the dysregulated mesentery blood vasculature as indicated by a significant reduction of vessel density, width, and branch points (Fig. 4F–H). The lymphatic vasculature density and the tortuosity and patent lumen of the

Published OnlineFirst October 15, 2015; DOI: 10.1158/0008-5472.CAN-14-3373

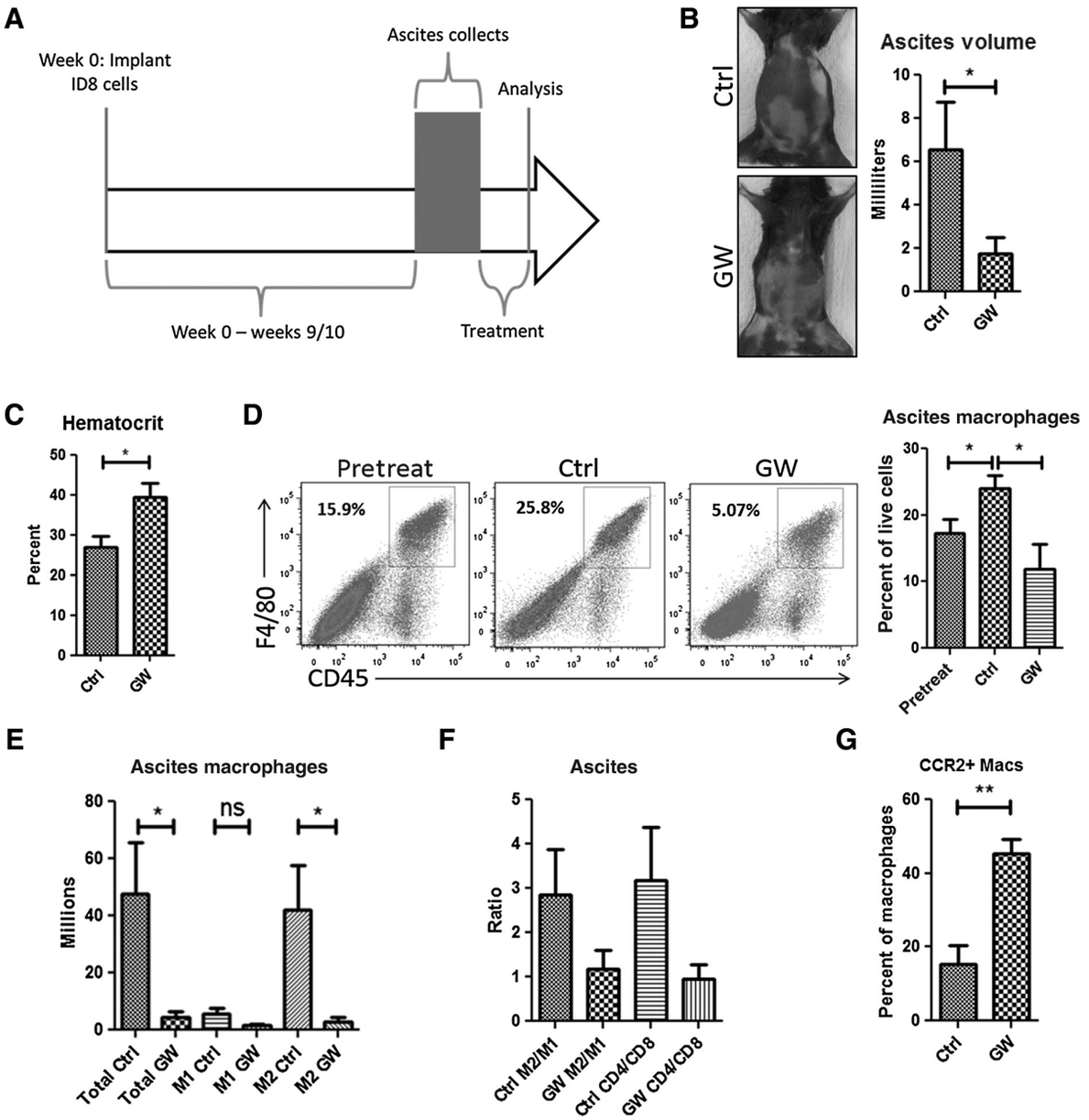

Figure 3.

CSF1R inhibition improves the health of mice-bearing ID8 EOC. A, ID8 cancer progression and GW2580 (GW) treatment timeline. B, CSF1R inhibition reduces ascites volume. Graph shows average ascites volume/animal ($n = 9$–10). C, hematocrit after 2 weeks of treatment ($n = 4$). D, content of macrophage in ascites before and after GW2580 treatment. Samples of ascites (<50 μL) drained immediately before or after a 2-week treatment course of vehicle or GW2580 were assessed for macrophage ($CD45^+$, $F4/80^+$) levels ($n = 3$). E, absolute numbers of total, M2 and M1 ascites macrophages with and without GW2580 treatment ($n = 3$–4). ns, nonsignificant. F, the M2:M1 macrophage ratios and CD4:CD8 T-cell ratios in control-treated and GW2580-treated ascites ($n = 7$–10). G, ascites macrophage CCR2 expression ($n = 3$). *, $P < 0.05$; **, $P < 0.01$.

lymphatics are all decreased with GW2580 treatment (Supplementary Fig. S3D and S3E).

To further assess the vascular leakage-causing potential of malignant ascites, we performed additional EC permeability assays with control or GW2580-treated mouse ascites sera. As shown in Fig. 5A, unlike normal murine blood serum that did not alter the (ECIS) EC permeability over 4 hours, the ascites serum from control (untreated) ID8 tumor-bearing animals induced a reduction in EC resistance, reaching a level that is about 15% to 20% below normal blood serum. In contrast, the addition of ascites sera from GW2580-treated mice resulted in an immediate increase in EC resistance reaching a level that is 15% higher than control mouse sera. Although the magnitude of change in EC resistance was not large, the direction of change was very consistent. Analyses on ascites sera from seven control and seven GW-treated mice across three different studies showed a significant

Published OnlineFirst October 15, 2015; DOI: 10.1158/0008-5472.CAN-14-3373

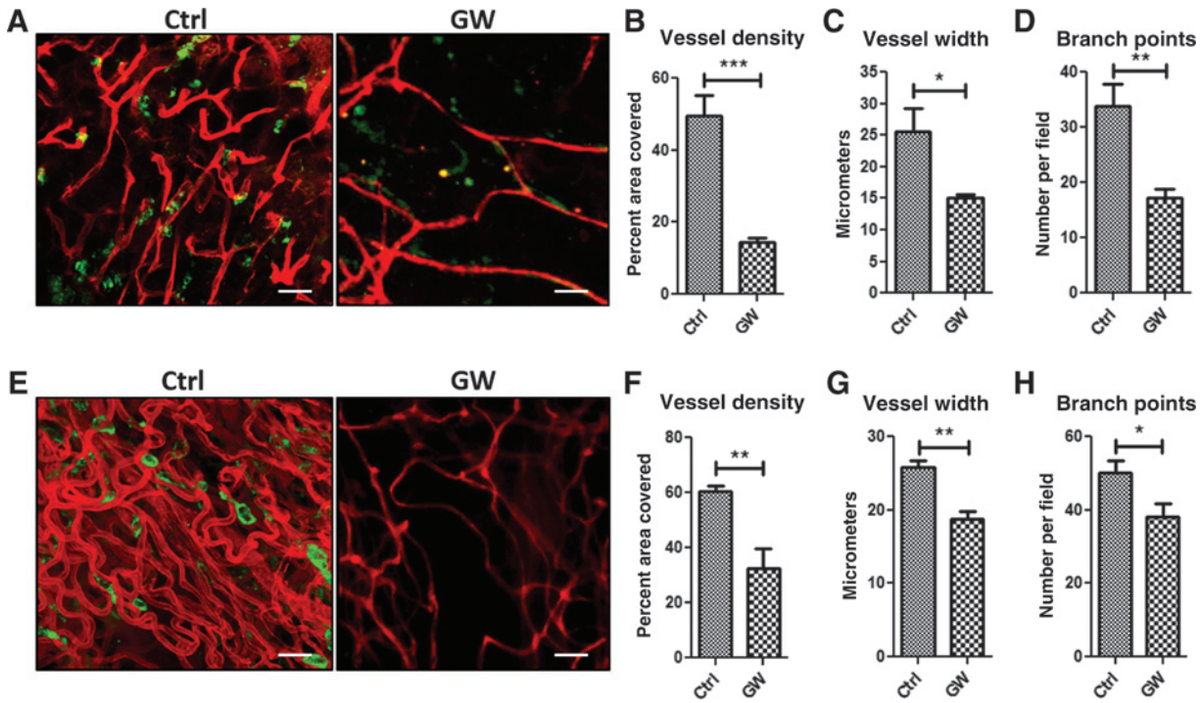

Figure 4.
CSF1R inhibition reduces vascular dysregulation in ID8 and OVCAR3 EOC. Mesentery vasculatures (isolectin, red) and macrophages (CD206$^+$, green) in control and GW2580-treated ID8-bearing animals (A) and OVCAR3-bearing animals (E), as assessed by staining of whole mount tissue. Vascular parameters (vessel density, vessel width, branch points) in ID8-bearing (B–D) and OVCAR3-bearing (F–H) animals ($n = 4$). Scale bars, 50 μm. *, $P < 0.05$; **, $P < 0.01$; ***, $P < 0.001$.

increase in EC resistance in the GW-treated over control mice (**, $P < 0.01$; Fig. 5B). Endothelial permeability is regulated by cell–cell adherens junctions, which are largely composed of vascular endothelial cadherin (37). The downregulation of this endothelium-specific cadherin from the plasma membrane of ECs leads to increased vascular permeability (38). The ability of ascites sera to induce endothelial permeability was further assessed by their impact on the surface VE-cadherin expression on the ECs. Incubating ECs with control (untreated) ascites serum led to a significant downregulation of VE-cadherin expression (relative to normal media), whereas GW-treated ascites did not significantly reduced VE-cadherin expression (Fig. 5C).

The improvement of *in vivo* vascular function upon CSF1R blockade was further verified by the significant increase in the number of perfused, blood-carrying capillaries (Fig. 5D) and the reduced vascular leakage assessed by the Miles assay (Fig. 5E) in the mesentery of GW2580-treated mice compared with that from the untreated control. Notably, the increased vascular leakage was largely limited to the tumor-bearing peritoneal compartment as no significant difference was observed in the muscles of naïve, control- or GW-treated animals (Supplementary Fig. S3F). Although VEGF is well-known to contribute to both blood and lymphatic vascular dysregulation in cancer, the vascular normalization observed with GW2580 treatment happened without a change in the very high VEGF levels observed in the ascites serum of ID8 EOC model (Supplementary Fig. S3G). This result suggests that other factor(s) may be counteracting the impact of VEGF as a result of the CSF1R blocking treatment.

Although the main focus here is to decipher the influences of myeloid cells/macrophages on malignant ascites, it is clear that the CSF1R blockade treatment has a major systemic impact. As shown in Supplementary Fig. S3, GW2580 treatment significantly reduced peripheral blood MDSCs (Supplementary Fig. S3H), spleen weight (Supplementary Fig. S3I), and splenic myeloid cells (Supplementary Fig. S3J), and macrophages in lymph nodes (Supplementary Fig. S3K). CSF1R blockade also significantly reduced TAMs in the tumor (Supplementary Fig. S3L). Similar to what was seen in the ID8 model, the TAMs in the OVCAR3 model showed significant polarization toward a less protumorigenic phenotype with GW2580 treatment (Supplementary Fig. S3M and S3N). This appeared to be due to an influx of the M1 macrophages upon treatment (Supplementary Fig. S3O). Of interest, the short 2-week GW2580 treatment appeared to reduce the overall intraperitoneal tumor burden in both the ID8 model (Supplementary Fig. S4A and S4B) and the OVCAR3 model (Supplementary Fig. S4C). In light of the same treatment having no effect on subcutaneous tumor burden (Supplementary Fig. S2E), we conclude that the ascites microenvironment becoming unfavorable for tumor growth could be the cause.

Increased macrophage presence in patient ascites predicts EC permeability

Next, we explored whether the macrophage findings in the murine models corroborate those in patients with EOC. In freshly isolated samples of ascites fluid from patients, macrophages and floating tumor cells again constituted the majority of viable cells in the ascites fluid (Fig. 6A). The M2 macrophages (CD33$^+$

Published OnlineFirst October 15, 2015; DOI: 10.1158/0008-5472.CAN-14-3373

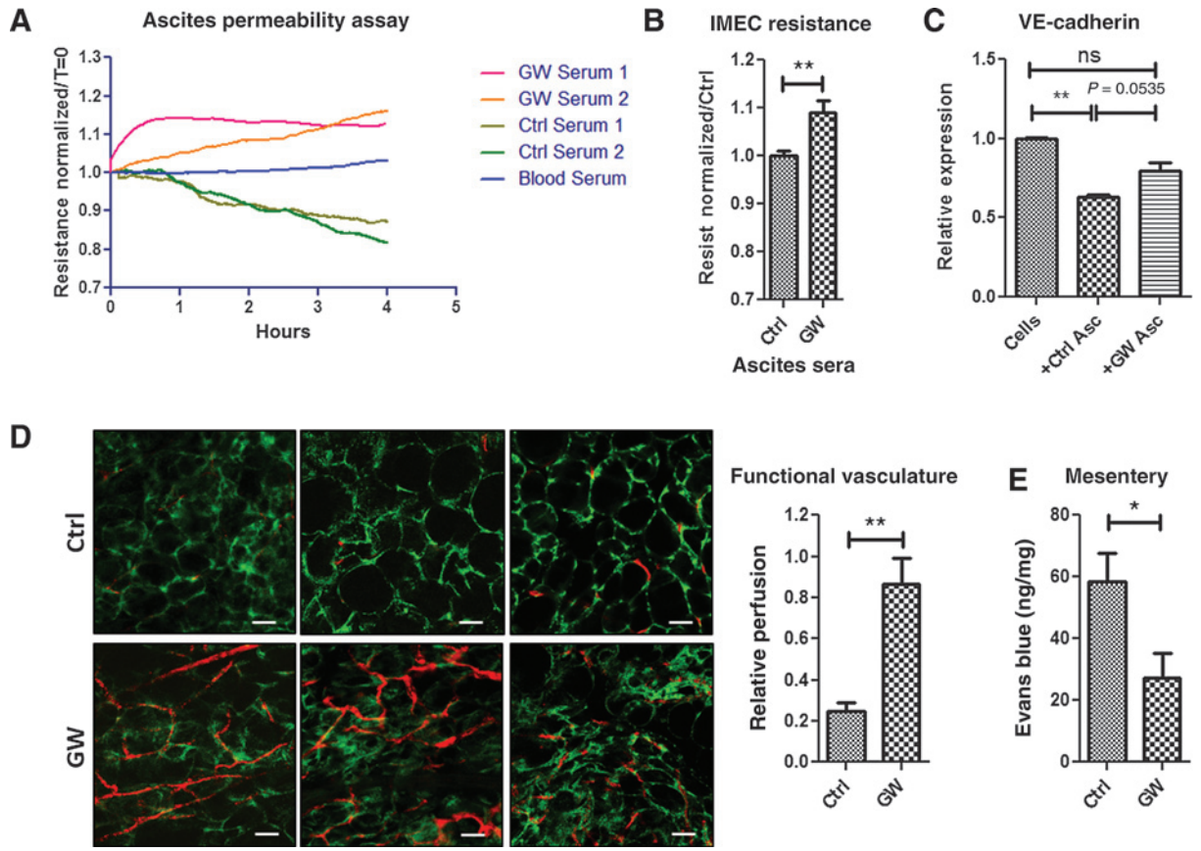

Figure 5.
CSF1R inhibition reduces vascular dysfunction in ID8 EOC. A, this graph shows five representative endothelial monolayers' resistance plotted over 4 hours. B, four-hour endothelial layer permeability assay of control versus GW-treated cell-free ascites sera ($n = 7$). C, VE-Cadherin expression in EC monolayers treated with ascites sera. D, vasculature function assay with perfused lectin (red) and surface stained CD31 (green) assessed by whole mount. Quantification is the percentage of $CD31^+$ vessels that are also lectin+ and normalized to naïve mouse vasculature ($n = 4$). E, vascular leakage Miles assay that quantified amount of Evans Blue in mesentery (ng dye/mg tissue; $n = 2$–3). Scale bars, 50 μm. *, $P < 0.05$; **, $P < 0.01$.

$CD68^+$ $MHCII^-$ $CD206^+$) outnumber the M1 macrophages ($CD33^+$ $CD68^+$ $MHCII^+$ $CD206^-$) by almost 3:1 and CD4 T cells outnumber CD8 T cells by more than 3:1 (Fig. 6B). Interestingly, the proportion and phenotype of the patients' ascites immune cells is almost identical to that of the ID8 model (Fig. 1B and C, Supplementary Fig. S5).

The ability of patients' ascites serum to induce vascular permeability of HUVECs was measured by the ECIS assay. Analyses on five patient ascites sera showed that the 2-hour mark represent the inflection point of this assay, where the EC resistance began to change (Fig. 6C). Interestingly, the macrophage content in the ascites (as % of live cells) significantly correlated with the inverse of EC resistance (Fig. 6D). In another words, the higher the number of macrophages in a patient's ascites, the higher the vascular permeability (i.e., loss of EC resistance) when the ascites serum is placed on ECs. These results from clinical specimens are suggestive of a pathological contribution of macrophages to vascular dysfunction, reminiscent of our findings in the murine models.

Collectively, the results from this therapeutic study support that protumorigenic macrophages are playing an instrumental role in the vascular dysfunction causing EOC malignant ascites. Inhibiting the macrophages' function with selective CSF1R blockade not only dramatically reversed the vascular pathology but also improved systematic environment that might be more favorable to reject the tumor. Thus, inhibiting the protumorigenic influences of myeloid cells/macrophages could be a part of a comprehensive treatment plan, to improve the outcome of EOC.

Discussion

Malignant ascites is a devastating complication of EOC that greatly lowers the quality of life of patients at late stages of the disease (2). Current treatment options for malignant ascites are largely ineffective and have high rate of complications (2). Recent research and results from clinical trials showed that VEGF is a promising therapeutic target, especially for malignant ascites (11–14). However, the notable risk of severe and even deadly side effects coupled with the lack of long-term survival benefits of VEGF-targeted therapies raised significant concern on their use. In this study, we postulate that broadening the therapeutic target to a particular immune cell population, namely macrophages, could be advantageous over VEGF-specific approaches. The protumorigenic TAMs are known to promote angiogenesis through VEGF dependent and independent means and heightening the immunosuppressive state of tumor microenvironment (16, 17). Thus,

Published OnlineFirst October 15, 2015; DOI: 10.1158/0008-5472.CAN-14-3373

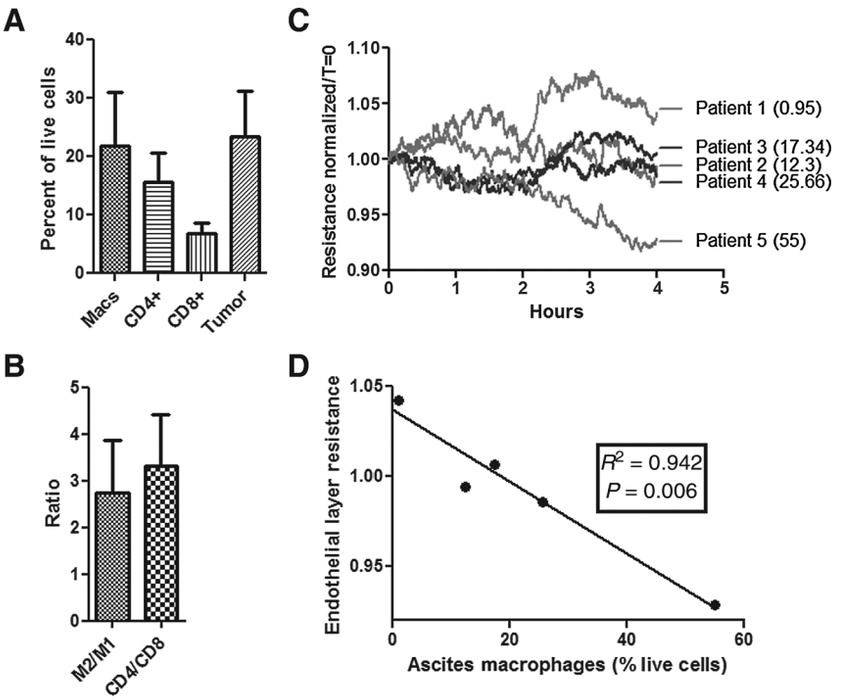

Figure 6.
EOC patient ascites and macrophages. A, EOC patient ascites cellular content is largely macrophages ($CD33^+$ $CD68^+$) and tumor cells ($CD33^-$ Muc-1^+; $n = 8$). B, the macrophages in patient ascites are largely "M2" tumor-promoting macrophages ($CD33^+$ $CD68^+$ $CD206^+$ HLA-DR^-) as opposed to the "M1" antitumor macrophages ($CD33^+$ $CD68^+$ $CD206^-$ HLA-DR^+), and $CD4^+$ T cells outnumber the $CD8^+$ T cells ($n = 6$). C, graph of HUVEC endothelial layer resistance over 4 hours during a permeability assay with patient ascites serum. Beside each patient number are parentheses with the percent of macrophages in that patient's ascites. D, the resistance at four hours (from C) correlated negatively with the macrophage content of the ascites ($n = 5$).

simultaneously blocking multiple prongs of TAMs' influences might be more effective than blocking the single VEGF axis.

Several high-impact studies published recently highlighted that CSF1R inhibition, by either monoclonal antibody or selective small molecule kinase inhibitors, can improve the outcome of different types of cancer in preclinical and clinical settings (39–42), by specifically reducing the protumorigenic M2 macrophage subtype and functions (40–42). The results of this study reinforce the same concept that selective blockade of CSF1R signaling reduces the number of M2 macrophages and their function, which reverses the vascular leakage of EOC malignant ascites. We observed higher macrophage content in human ascites sera was associated with increased vascular permeability. In murine EOC models, M2 macrophages expanded and infiltrated the peritoneal vasculature over time and were linked to progressive vascular dysregulation, leaky vessels, and ascites formation. Using a well-studied selective CSF1R inhibitor, GW2580, (33–36, 43) to block macrophage function in late stages of EOC reversed the vascular dysfunction and greatly reduced ascites accumulation. We deduce that the vascular normalization is secondary to the lowered M2 macrophage contributions as the reduction of total macrophages in ascites after GW2580 treatment was predominantly due to reductions in the MHC-negative M2 population, whereas M1 macrophages are affected less appreciably. Consequently, GW2580 treatment significantly increased the proportion of M1 macrophages, expressing CCR2, IL12, and IFNγ. Furthermore, the improvement of macrophage polarization status was accompanied by an increase of the CD8/CD4 T-cell ratio and hence, lowering the immunosuppressive state of tumor microenvironment, as observed in recent studies (30, 42). In total, these recent findings all support that selective CSF1R inhibition can improve cancer outcome by lowering the protumorigenic activities of M2 macrophages, which promotes the vascular dysregulation of EOC malignant ascites reported here.

We deduced that one component of the macrophage-mediated vascular dysfunction is dictated through soluble factors as cell-free ascites sera from untreated animals induced higher EC permeability. In this exploratory study, we did not address the specific soluble factor(s) induced by macrophages that might be promoting or protecting vascular permeability in malignant ascites of EOC. However, we believe VEGF is not the culprit. VEGF protein levels in the ID8 ascites is very high, several orders of magnitude higher than in peripheral blood. In GW2580-treated ascites sera, VEGF levels remained very high, often exceeding that of untreated sera. It is interesting to note that ascites serum from GW2580-treated mice consistently induced a higher EC resistance when compared with normal blood serum. This result could indicate the presence of a protective factor(s) against vascular leak in the GW-treated sera, especially to counteract the permeability effects of VEGF.

Another layer of complexity in this macrophage-induced vascular dysfunction is the close cell–cell contact and cross-talk between macrophages and EC cells that have been reported in developmental and pathological settings. Our recent study showed that ECs provide a specific niche for the proliferation and differentiation of macrophages (44) and macrophages are often recruited to sites of vascular remodeling during embryonic development (45). Kubota and colleagues (46) showed that macrophages play a key role in pathological neovascularization of ischemic retinopathy. Reduction of the macrophages' number and function either by genetic deletion of CSF-1 (M-CSF) or by a CSF1R (c-fms) kinase inhibitor, Ki20227, was able to correct the vascular pathology. In oncology, physical interactions between macrophages and endothelial cells has been described in the context of breast cancer metastasis facilitation (47, 48). Clearly, the functional cross-talk between macrophages and ECs is an important topic in cancer and vascular biology.

Published OnlineFirst October 15, 2015; DOI: 10.1158/0008-5472.CAN-14-3373

Although the precise molecular mechanism of the macrophage-driven vascular dysfunction is yet to be determined, our results support that therapies that inhibit macrophage functions will be a rational strategy to manage ascites. Because CSF1/CSF1R is a dominant driver pathway in the function of TAMs, it is a promising target and there is a wealth of pharmacological agents available to inhibit this axis. For instance, selective monoclonal antibodies that target either the ligand or the receptor, and numerous small molecule CSF1R tyrosine kinase inhibitors, exhibiting variable target selectivity, have been developed in the last 10 years (33, 39–41). Many of these agents are in early phase clinical investigation for inflammatory diseases and cancer. The CSF1R inhibitor PLX3397 is the furthest along in clinical testing, especially in oncology application (39). Paralleling our finding that daily oral GW2580 regimen (160 mg/kg) given to mice over 1 month resulted in no discernable toxicity, early clinical trial findings showed that PLX3397 appeared to be well tolerated in patients with advanced cancer (39).

Recent therapeutic developments for EOC favored intraperitoneal-directed cisplatin delivery as this route was shown to prolong the survival of patients over systemic delivery (49). We believe that it might not be beneficial to administer the TAMs blockade therapy described here by intraperitoneal route even though it is directed mainly to relieve a peritoneal-based complication. Recent reports published by our group and others demonstrated that the benefit of inhibiting TAMs infiltration and function is systemic and not tumor or tissue-confined as this treatment can greatly improve the outcomes of conventional cancer therapies, such as antiangiogenesis therapy, radiotherapy, chemotherapy, and vaccine therapy in prostate cancers (34, 35), lung cancers, and breast cancers (30). Here, we showed that CSF1R blockade resulted in systemic reduction of immunosuppressive MDSCs and thus lowering the tumor supportive environment, which in turn could contribute to the lowered tumor burden observed. Given these promising findings, the combination of TAMs blockade with conventional chemotherapy treatment might be particular fruitful for EOC.

Given the very heterogeneous nature of human EOC and the known plasticity of myeloid cell and macrophage subtypes in cancer, a critical issue for clinical translation of TAM blockade strategy is to determine which patients might be responsive to CSF1/CSF1R-targeted or other TAM-targeted therapy. Clearly, the promising prospects of this therapeutic strategy warrant more study and attention pay to myeloid cells' contribution to the aggressive and resistant nature of EOC. This knowledge could lead to more rationale therapeutic strategies to improve the current poor outcome for EOC.

Disclosure of Potential Conflicts of Interest

No potential conflicts of interest were disclosed.

Authors' Contributions

Conception and design: D.L. Moughon, S. Schokrpur, J. David, M.L. Iruela-Arispe, O. Dorigo, L. Wu

Development of methodology: D.L. Moughon, C. Lin, O. Dorigo

Acquisition of data (provided animals, acquired and managed patients, provided facilities, etc.): H. He, Z.K. Jiang, M. Yaqoob, J. David, O. Dorigo

Analysis and interpretation of data (e.g., statistical analysis, biostatistics, computational analysis): D.L. Moughon, H. He, S. Schokrpur, J. David, O. Dorigo

Writing, review, and/or revision of the manuscript: D.L. Moughon, H. He, S. Schokrpur, O. Dorigo, L. Wu

Administrative, technical, or material support (i.e., reporting or organizing data, constructing databases): H. He, L. Wu

Study supervision: O. Dorigo, L. Wu

Acknowledgments

The authors thank Dr. Wafic ElMasri, Caroline Hillerup, and Dr. Chintda Santiskulvong for patient sample procurement, Carol Eng for animal experimentation, and Ryan Freshman for technical support. The authors also thank the faculty and staff of the UCLA Crump Institute for Molecular Imaging for technical support and help. This work was supported by the CDMRP Ovarian Cancer Research Program grant W81XWH-11-1-0804 (L. Wu and O. Dorigo), the UCLA Jonsson Comprehensive Cancer Center Transdisciplinary Grant (L. Wu, O. Dorigo, and M.L. Iruela-Arispe) as part of the NIH/NCATS Grant #UL1TR000124. D.L. Moughon was supported by Tumor Immunology Training Grant (T32-CA009120-35), the Tumor Cell Biology Training Grant (T32 CA009056), and the Vascular Biology Training Grant (T32HL69766).

The costs of publication of this article were defrayed in part by the payment of page charges. This article must therefore be hereby marked *advertisement* in accordance with 18 U.S.C. Section 1734 solely to indicate this fact.

Received November 18, 2014; revised August 14, 2015; accepted August 23, 2015; published OnlineFirst October 15, 2015.

References

1. Chung M, Kozuch P. Treatment of malignant ascites. Curr Treat Options Oncol 2008;9:215–33.
2. Eskander RN, Tewari KS. Emerging treatment options for management of malignant ascites in patients with ovarian cancer. Int J Womens Health 2012;4:395–404.
3. Kipps E, Tan DSP, Kaye SB. Meeting the challenge of ascites in ovarian cancer: new avenues for therapy and research. Nat Rev Cancer 2013;13:273–82.
4. Kobold S, Hegewisch-Becker S, Oechsle K, Jordan K, Bokemeyer C, Atanackovic D. Intraperitoneal VEGF inhibition using bevacizumab: a potential approach for the symptomatic treatment of malignant ascites? Oncologist 2009;14:1242–51.
5. Senger DR, Galli SJ, Dvorak AM, Perruzzi CA, Harvey VS, Dvorak HF. Tumor cells secrete a vascular permeability factor that promotes accumulation of ascites fluid. Science 1983;219:983–5.
6. Zebrowski BK, Liu W, Ramirez K, Akagi Y, Mills GB, Ellis LM. Markedly elevated levels of vascular endothelial growth factor in malignant ascites. Ann Surg Oncol 1999;6:373–8.
7. Santin AD, Hermonat PL, Ravaggi A, Cannon MJ, Pecorelli S, Parham GP. Secretion of vascular endothelial growth factor in ovarian cancer. Eur J Gynaecol Oncol 1999;20:177–81.
8. Paley PJ, Staskus KA, Gebhard K, Mohanraj D, Twiggs LB, Carson LF, et al. Vascular endothelial growth factor expression in early stage ovarian carcinoma. Cancer 1997;80:98–106.
9. Cooper BC, Ritchie JM, Broghammer CLW, Coffin J, Sorosky JI, Buller RE, et al. Preoperative serum vascular endothelial growth factor levels: significance in ovarian cancer. Clin Cancer Res 2002;8:3193–7.
10. Hefler LA, Zeillinger R, Grimm C, Sood AK, Cheng WF, Gadducci A, et al. Preoperative serum vascular endothelial growth factor as a prognostic parameter in ovarian cancer. Gynecol Oncol 2006;103:512–7.
11. Byrne AT, Ross L, Holash J, Nakanishi M, Hu L, Hofmann JI, et al. Vascular endothelial growth factor-trap decreases tumor burden, inhibits ascites, and causes dramatic vascular remodeling in an ovarian cancer model. Clin Cancer Res 2003;9:5721–8.
12. Hu L, Hofmann J, Holash J, Yancopoulos GD, Sood AK, Jaffe RB. Vascular endothelial growth factor trap combined with paclitaxel strikingly inhibits tumor and ascites, prolonging survival in a human ovarian cancer model. Clin Cancer Res 2005;11:6966–71.
13. Colombo N, Mangili G, Mammoliti S, Kalling M, Tholander B, Sternas L, et al. A phase II study of aflibercept in patients with advanced epithelial

Published OnlineFirst October 15, 2015; DOI: 10.1158/0008-5472.CAN-14-3373

ovarian cancer and symptomatic malignant ascites. Gynecol Oncol 2012;125:42–7.
14. Gotlieb WH, Amant F, Advani S, Goswami C, Hirte H, Provencher D, et al. Intravenous aflibercept for treatment of recurrent symptomatic malignant ascites in patients with advanced ovarian cancer: a phase 2, randomised, double-blind, placebo-controlled study. Lancet Oncol 2012;13:154–62.
15. Han ES, Monk BJ. What is the risk of bowel perforation associated with bevacizumab therapy in ovarian cancer? Gynecol Oncol 2007;105:3–6.
16. Qian B-Z, Pollard JW. Macrophage diversity enhances tumor progression and metastasis. Cell 2010;141:39–51.
17. De Palma M, Lewis CE. Macrophage regulation of tumor responses to anticancer therapies. Cancer Cell 2013;23:277–86.
18. Reinartz S, Schumann T, Finkernagel F, Wortmann A, Jansen JM, Meissner W, et al. Mixed-polarization phenotype of ascites-associated macrophages in human ovarian carcinoma: correlation of CD163 expression, cytokine levels and early relapse. Int J Cancer 2014;134:32–42.
19. Takaishi K, Komohara Y, Tashiro H, Ohtake H, Nakagawa T, Katabuchi H, et al. Involvement of M2-polarized macrophages in the ascites from advanced epithelial ovarian carcinoma in tumor progression via Stat3 activation. Cancer Sci 2010;101:2128–36.
20. Mouchemore KA, Pixley FJ. CSF-1 signaling in macrophages: pleiotrophy through phosphotyrosine-based signaling pathways. Crit Rev Clin Lab Sci 2012;49:49–61.
21. Verreck FAW, de Boer T, Langenberg DML, Hoeve MA, Kramer M, Vaisberg E, et al. Human IL-23-producing type 1 macrophages promote but IL-10-producing type 2 macrophages subvert immunity to (myco)bacteria. Proc Natl Acad Sci U S A 2004;101:4560–5.
22. Martinez FO, Gordon S, Locati M, Mantovani A. Transcriptional profiling of the human monocyte-to-macrophage differentiation and polarization: new molecules and patterns of gene expression. J Immunol 2006;177:7303–11.
23. Chambers SK. Role of CSF-1 in progression of epithelial ovarian cancer. Future Oncol Lond Engl 2009;5:1429–40.
24. Price FV, Chambers SK, Chambers JT, Carcangiu ML, Schwartz PE, Kohorn EI, et al. Colony-stimulating factor-1 in primary ascites of ovarian cancer is a significant predictor of survival. Am J Obstet Gynecol 1993;168:520–7.
25. Brakenhielm E, Burton JB, Johnson M, Chavarria N, Morizono K, Chen I, et al. Modulating metastasis by a lymphangiogenic switch in prostate cancer. Int J Cancer 2007;121:2153–61.
26. Roby KF, Taylor CC, Sweetwood JP, Cheng Y, Pace JL, Tawfik O, et al. Development of a syngeneic mouse model for events related to ovarian cancer. Carcinogenesis 2000;21:585–91.
27. Peter S, Bak G, Hart K, Berwin B. Ovarian tumor-induced T cell suppression is alleviated by vascular leukocyte depletion. Transl Oncol 2009;2:291–9.
28. Leinster DA, Colom B, Whiteford JR, Ennis DP, Lockley M, McNeish IA, et al. Endothelial cell junctional adhesion molecule C plays a key role in the development of tumors in a murine model of ovarian cancer. FASEB J 2013;27:4244–53.
29. Almand B, Clark JI, Nikitina E, van Beynen J, English NR, Knight SC, et al. Increased production of immature myeloid cells in cancer patients: a mechanism of immunosuppression in cancer. J Immunol Baltim Md 1950 2001;166:678–89.
30. DeNardo DG, Brennan DJ, Rexhepaj E, Ruffell B, Shiao SL, Madden SF, et al. Leukocyte complexity predicts breast cancer survival and functionally regulates response to chemotherapy. Cancer Discov 2011;1:54–67.
31. Jeon B-H, Jang C, Han J, Kataru RP, Piao L, Jung K, et al. Profound but dysfunctional lymphangiogenesis via vascular endothelial growth factor ligands from CD11b+ macrophages in advanced ovarian cancer. Cancer Res 2008;68:1100–9.
32. Liao S, Liu J, Lin P, Shi T, Jain RK, Xu L. TGF-beta blockade controls ascites by preventing abnormalization of lymphatic vessels in orthotopic human ovarian carcinoma models. Clin Cancer Res 2011;17:1415–24.
33. Conway JG, McDonald B, Parham J, Keith B, Rusnak DW, Shaw E, et al. Inhibition of colony-stimulating-factor-1 signaling in vivo with the orally bioavailable cFMS kinase inhibitor GW2580. Proc Natl Acad Sci U S A 2005;102:16078–83.
34. Priceman SJ, Sung JL, Shaposhnik Z, Burton JB, Torres-Collado AX, Moughon DL, et al. Targeting distinct tumor-infiltrating myeloid cells by inhibiting CSF-1 receptor: combating tumor evasion of antiangiogenic therapy. Blood 2010;115:1461–71.
35. Xu J, Escamilla J, Mok S, David J, Priceman S, West B, et al. CSF1R signaling blockade stanches tumor-infiltrating myeloid cells and improves the efficacy of radiotherapy in prostate cancer. Cancer Res 2013;73:2782–94.
36. Escamilla J, Schokrpur S, Liu C, Priceman SJ, Moughon D, Jiang Z, et al. CSF1 receptor targeting in prostate cancer reverses macrophage-mediated resistance to androgen blockade therapy. Cancer Res 2015;75:950–62.
37. Dejana E, Orsenigo F, Lampugnani MG. The role of adherens junctions and VE-cadherin in the control of vascular permeability. J Cell Sci 2008;121:2115.
38. Gavard J, Gutkind JS. VEGF controls endothelial-cell permeability by promoting the β-arrestin-dependent endocytosis of VE-cadherin. Nat Cell Biol 2006;8:1223–34.
39. Tap WD, Wainberg ZA, Anthony SP, Ibrahim PN, Zhang C, Healey JH, et al. Structure-guided blockade of CSF1R kinase in tenosynovial giant-cell tumor. N Engl J Med 2015;373:428–37.
40. Pyonteck SM, Akkari L, Schuhmacher AJ, Bowman RL, Sevenich L, Quail DF, et al. CSF-1R inhibition alters macrophage polarization and blocks glioma progression. Nat Med 2013;19:1264–72.
41. Cassier PA, Italiano A, Gomez-Roca CA, Le Tourneau C, Toulmonde M, Cannarile MA, et al. CSF1R inhibition with emactuzumab in locally advanced diffuse-type tenosynovial giant cell tumours of the soft tissue: a dose-escalation and dose-expansion phase 1 study. Lancet Oncol 2015;16:949–56.
42. Ries CH, Cannarile MA, Hoves S, Benz J, Wartha K, Runza V, et al. Targeting tumor-associated macrophages with anti-CSF-1R antibody reveals a strategy for cancer therapy. Cancer Cell 2014;25:846–59.
43. Karaman MW, Herrgard S, Treiber DK, Gallant P, Atteridge CE, Campbell BT, et al. A quantitative analysis of kinase inhibitor selectivity. Nat Biotechnol 2008;26:127–32.
44. He H, Xu J, Warren CM, Duan D, Li X, Wu L, et al. Endothelial cells provide an instructive niche for the differentiation and functional polarization of M2-like macrophages. Blood 2012;120:3152–62.
45. Al-Roubaie S, Hughes JH, Filla MB, Lansford R, Lehoux S, Jones EAV. Time-lapse microscopy of macrophages during embryonic vascular development. Dev Dyn 2012;241:1423–31.
46. Kubota Y, Takubo K, Shimizu T, Ohno H, Kishi K, Shibuya M, et al. M-CSF inhibition selectively targets pathological angiogenesis and lymphangiogenesis. J Exp Med 2009;206:1089–102.
47. Robinson BD, Sica GL, Liu Y-F, Rohan TE, Gertler FB, Condeelis JS, et al. Tumor microenvironment of metastasis in human breast carcinoma: a potential prognostic marker linked to hematogenous dissemination. Clin Cancer Res 2009;15:2433–41.
48. Wyckoff JB, Wang Y, Lin EY, Li J, Goswami S, Stanley ER, et al. Direct visualization of macrophage-assisted tumor cell intravasation in mammary tumors. Cancer Res 2007;67:2649–56.
49. Armstrong DK, Bundy B, Wenzel L, Huang HQ, Baergen R, Lele S, et al. Intraperitoneal cisplatin and paclitaxel in ovarian cancer. N Engl J Med 2006;354:34–43.

Published OnlineFirst October 15, 2015; DOI: 10.1158/0008-5472.CAN-14-3373

Cancer Research
The Journal of Cancer Research (1916–1930) | The American Journal of Cancer (1931–1940)

AACR American Association for Cancer Research

Macrophage Blockade Using CSF1R Inhibitors Reverses the Vascular Leakage Underlying Malignant Ascites in Late-Stage Epithelial Ovarian Cancer

Diana L. Moughon, Huanhuan He, Shiruyeh Schokrpur, et al.

Cancer Res 2015;75:4742-4752. Published OnlineFirst October 15, 2015.